available at www.sciencedirect.com

ScienceDirect

journal homepage: www.elsevier.com/locate/ijrefrig

Design optimization of scroll compressor applied for frictional losses evaluation

Yangguang Liu [a], Chinghua Hung [a,*], Yuchoung Chang [b]

[a] Department of Mechanical Engineering, National Chiao Tung University, EE452, 1001 Ta Hsueh Road, Hsinchu 300, Taiwan
[b] Energy & Environment Research Laboratories, Industrial Technology Research Institute, Taiwan

ARTICLE INFO

Article history:
Received 13 February 2009
Received in revised form
12 October 2009
Accepted 14 December 2009
Available online 28 December 2009

Keywords:
Scroll compressor
Modelling
Simulation
Loss
Friction

ABSTRACT

This paper develops a design optimization procedure in scroll-type compressor (STC). By integrating the verified STC simulation model with an optimum solver, a frictional losses reduced problem of bearing components has been investigated. After the optimum search, the frictional losses can be reduced in range of 14.1–18.1% at all testing conditions with specified constraints. Herein, the design modifications of crank and upper bearings are compromised between reduction of frictional losses and maintenance of hydrodynamic lubrication. In addition, the narrower and shorter design of lower bearing and smaller one of thrust bearing can reduce frictional losses too. Furthermore, wider selection of materials in all the bearings can be adopted with the satisfied strength constraint. By using this procedure, various optimum combinations of parameters can be found for different STC design considerations.

Optimisation du compresseur à spirale appliqué à l'évaluation des pertes dues au frottement

Mots clés : Compresseur à spirale ; Modèlisation ; Simulation ; Perte ; Frottement

1. Introduction

The scroll-type compressor (STC), one kind of positive displacement compressor, has been well-developed due to advantages of higher efficiency, quiet operation and good reliability. Numerous literatures about STC had been published since 1980s. Among those, the mathematical model including geometrical characteristics, kinematics and dynamics has been disclosed (Morishita et al., 1984, 1986). The compression and discharge processes, leakage through clearances and superheat of suction pipe in thermodynamics also have been developed by Nieter and Gagne (1992); Schein and Radermacher (2001) and Chen et al. (2002). In addition, a comprehensive computer package integrated with above models has been constructed and verified with experimental test (Chang et al., 2004).

In viewpoint of optimum design, Etemad and Nieter (1989) have provided simple design approach to decide characteristic parameters within manufacturing limitations of STC. The

* *Corresponding author*. Tel.: +886 3 5712121x55160; fax: +886 3 5720634.
E-mail addresses: ygliu.me94g@nctu.edu.tw (Y. Liu), chhung@mail.nctu.edu.tw (C. Hung).
0140-7007/$ – see front matter © 2010 Elsevier Ltd and IIR. All rights reserved.
doi:10.1016/j.ijrefrig.2009.12.015

Nomenclature

C	clearance (mm)
D	diameter (mm)
$D_{i,th}$, $D_{o,th}$	inner and outer diameter of thrust bearing (mm)
F	force (N)
G	refrigerant mass flow rate (kg s^{-1})
h	wrap height (mm)
H, H_0	oil-film clearance (mm); nominal oil-film clearance (mm)
L	length (mm)
m_{ob}	mass of orbiting scroll (kg)
M	moment (N m)
N	turn number of scrolls
p, P	pressure (MPa); power (watt)
p_t	pitch of scroll (mm)
r_b, r_{ob}	basic radius (mm); orbiting radius (mm)
t, t_h	time (s); thickness (mm)
U	surface velocity (m s^{-1})
x, y	coordinate
R,Θ	cylindrical coordinate
α	tilting angle (rad)
β	directional turning angle (rad)
δ_e,δ_f	end-side clearance and flank clearance (m)
ε	eccentricity ratio
κ	initial angle of involute (rad)
ϕ	involute angle of scroll (rad)
Φ	phase difference (rad)
θ	orbiting angle of scroll (rad)
ω	angular velocity (rad s^{-1})
μ	viscosity (Pa s)
η_C,η_V	compressor efficiency, volumetric efficiency

Subscripts

a	axial direction
b	bearing
back	back side
b,cr	crank journal bearing
b,low	lower journal bearing
b,upp	upper journal bearing
c,csh	centrifugal direction of crank shaft
c,lcw	centrifugal direction of lower counterweight
c,ob	centrifugal direction of orbiting scroll
c,ucw	centrifugal direction of upper counterweight
dis	discharge
e	end-side
f,b, f,th	friction of the journal and thrust bearing
fi, i, fi,o	inner and outer involute of fixed scroll
i, j, k	index number
r	radial direction
scr	locus of the turning moment
suc	suction
θ	tangential direction

optimum combinations of two characteristic parameters, base circle radius and wrap height in STC for higher efficiency have been investigated by Ishii et al. (1992); Ishii et al. (1994, 1996). In addition, Tseng and Chang (2006) have used a systematic design procedure to develop a family optimization of STC products with high percentage of share in major components. For different compressor type, Ooi (2005) has presented a study combining the parametric simulation model with iterative optimum algorithm to develop design optimization in rolling piston compressor. However, that kind of application to STC was rarely discussed in literatures.

This paper proposes to develop a design optimization procedure by integrating the parametric STC model with an optimum solver "*MOST*" (Tseng, 1996). One case riveted on reduction of the frictional losses for bearing components in STC and investigation of relevant effects, are analyzed and discussed for demonstrating the optimization procedure.

2. Mathematical models of STC

The complete mathematical models of STC included geometry of the scroll, thermodynamics process, dynamic balance and frictional losses of mechanical components. Some simplified assumptions are employed in those models:

(1) Symmetric working chambers of the scroll pairs with homogeneous refrigerant are considered.
(2) Gravitational, kinetic energy variations are neglected.

2.1. *Geometrical model of scrolls*

One pair of scrolls is created by an involute profile with base circle. Equations of the fixed scroll can be written as follow:

$$\begin{aligned} x_{fi,o} &= r_b[\cos\phi + (\phi+\kappa)\sin\phi] \\ y_{fi,o} &= r_b[\sin\phi - (\phi+\kappa)\cos\phi] \end{aligned} \tag{1}$$

$$\begin{aligned} x_{fi,i} &= r_b[\cos\phi + (\phi-\kappa)\sin\phi] \\ y_{fi,i} &= r_b[\sin\phi - (\phi-\kappa)\cos\phi] \end{aligned} \tag{2}$$

The relation between orbiting scroll and fixed scroll can be derived by coordinate transformation. Some parameters used in the model are defined firstly as follows:

$$\begin{cases} r_b\text{: radius of base circle} \\ r_b = \dfrac{p_t}{2\pi} \end{cases};\ \begin{cases} \kappa\text{ : intial angle of involute} \\ \kappa = \dfrac{t_h}{2r_b} \end{cases};\ \begin{cases} r_{ob}\text{ : orbiting radius} \\ r_{ob} = \dfrac{p_t}{2} - t_h \end{cases}$$
$$\begin{cases} N\text{: number of chambers} \\ N = \mathrm{Int}\left(\dfrac{(\phi_e - \phi_{dis})}{2\pi}\right) + 1 \\ \phi_{dis}\text{: the discharged involute angle decided by cutting condition} \end{cases}$$
$$\begin{cases} \theta_{dis}\text{: discharged orbiting angle at one revolutation} \\ \theta_{dis} = (\phi_e - \phi_{dis}) - 2\pi\cdot(N-1) \end{cases} \tag{3}$$

The details to fundamental formulas adopted in the study, comprised calculation of the suction volume, compression volume of individual chambers during one orbiting cycle and discharge volume, has been derived by Morishita et al. (1984), Morishita et al. (1986) and Nieter and Gagne (1992).

2.2. Thermodynamic model of scrolls

For refrigerant property, the dynamic link library "*REFPROP 7*" (Lemmon et al., 2002) is integrated into the model. The thermodynamics including suction superheat, the compression and discharge with variations in pressure and temperature by polytropic process is considered. In addition, the leakage clearances of the scroll pair including the end-side and flank leakage, are dynamically and linearly linked to pressure ratio and back-pressure (Chen et al., 2002), and those linear functions can be represented as follows

$$\begin{aligned}\delta_e &= \left[0.85 \times \left(\frac{p_{dis}-p_{back}}{p_{suc}}\right)+1.65\right]\times 10^{-6}\\ \delta_f &= \left[-6.11 \times \left(\frac{p_{dis}-p_{back}}{p_{suc}}\right)+32\right]\times 10^{-6}\end{aligned} \tag{4}$$

For those leakages, one dimensional isentropic compressible flow in a nozzle (Chen et al., 2002 and Park et al., 2002) is used to derive the leakage mass flow rate.

2.3. Dynamics of mechanical components

The dynamic model of the orbiting scroll coupled with the Oldham ring (Morishita et al., 1984) is adopted in this study. Several dynamic forces caused by gas pressure in chambers and acted on the orbiting scroll are considered. Those forces are classified as tangential, radial and axial ones. As shown in Fig. 1(a), the tangential force (F_θ) and radial force (F_r) can be expressed as follows:

$$F_\theta = \sum_{i=1}^{N} F_{\theta i} = \sum_{i=1}^{N} r_b \cdot h \cdot (2\phi - \pi)\cdot(p_i - p_{i+1}) \tag{5}$$

$$F_r = \sum_{i=1}^{N} F_{ri} = \sum_{i=1}^{N} 2\cdot r_b \cdot h \cdot (p_i - p_{i+1}) \tag{6}$$

In axial direction, the back-pressure mechanism is used to reduce the axial load and the resultant axial force is

$$F_a = \sum_{i=1}^{N} p_i \cdot A_i - F_{back} + m_{ob}\cdot g \tag{7}$$

where A_i represented the chamber area derived by Morishita et al. (1986). Moreover, by neglecting the inertial force with constant speed consideration, the centrifugal force of the orbiting scroll is

$$F_{c,ob} = m_{ob}\cdot r_{ob}\cdot\left(\frac{d\theta}{dt}\right)^2 \tag{8}$$

The force and moment equations of the orbiting scroll coupled with Oldham ring are used to derive the bearing force of the crank journal bearing ($F_{b,cr}$) set up on the crank shaft (Morishita et al., 1984). Furthermore, by assuming the resultant axial force (F_a) and turning moment (M) must be balanced by reaction components resulted from the thrust surface (Morishita et al., 1984), the turning moment M and the directional turning angle β of the orbiting scroll can be shown as follows:

$$\begin{cases} M_x = F_a\cdot(y_{scr} - r_{ob}\sin\theta) \\ M_y = F_a\cdot(x_{scr} + r_{ob}\cos\theta) \end{cases};\quad M = \sqrt{M_x^2 + M_y^2}$$
$$\beta = \tan^{-1}\left(\frac{M_y}{M_x}\right) \tag{9}$$

(x_{scr},y_{scr}) represents the locus of the turning moment on the thrust surface.

Another important part is the counterweight analysis. Fig. 1(b) is the force diagram in x-direction, the crank bearing force ($F_{b,cr}$) and the centrifugal forces from the crank shaft ($F_{c,csh}$), the upper and lower counterweights ($F_{c,ucw}$ & $F_{c,lcw}$) are considered. The upper and lower journal bearings are used to support the driving shaft. By assuming the center of the upper

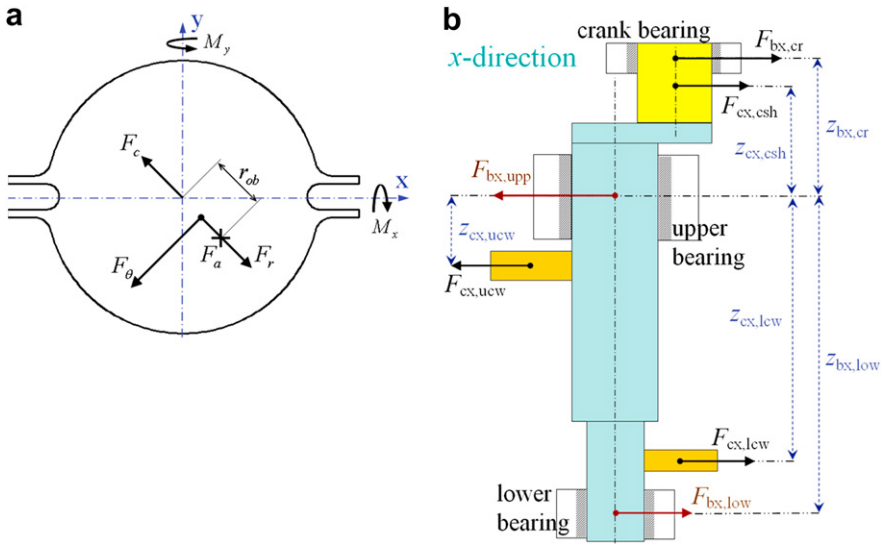

Fig. 1 – Illustrations of the dynamics (a) dynamic forces of the orbiting scroll (b) dynamic balance of the driving shaft.

journal bearing as the pivot, the two bearing forces can be derived as follows

$$\begin{cases} F_{bx,low}\cdot z_{bx,low} = F_{bx,cr}\cdot z_{bx,cr} + F_{cx,csh}\cdot z_{cx,csh} + F_{cx,ucw}\cdot z_{cx,ucw} - F_{cx,lcw}\cdot z_{cx,lcw} \\ F_{by,low}\cdot z_{by,low} = F_{by,cr}\cdot z_{by,cr} + F_{cy,csh}\cdot z_{cy,csh} + F_{cy,ucw}\cdot z_{cy,ucw} - F_{cy,lcw}\cdot z_{cy,lcw} \\ F_{bx,upp} + F_{cx,ucw} = F_{bx,cr} + F_{cx,csh} + F_{bx,low} + F_{cx,lcw} \\ F_{by,low} + F_{cy,ucw} = F_{by,cr} + F_{cy,csh} + F_{by,low} + F_{cy,lcw} \end{cases} \quad (10)$$
$$F_{b,low} = \sqrt{F_{bx,low}{}^2 + F_{by,low}{}^2}; \quad F_{b,upp} = \sqrt{F_{bx,upp}{}^2 + F_{by,upp}{}^2}$$

2.4. Frictional losses in mechanical components

In addition to the compression power consumed during STC operation, other main expenses are the frictional losses from the mechanical components. Those losses are mainly caused from the thrust surface (as thrust bearing) and the three journal bearings. In addition, by assuming the frictional losses around the other mechanical components (such as Oldham ring) is negligibly small compared with the bearing losses (Ishii et al., 1994), the frictional coefficient of the other mechanical components is set as 0.013 (Ishii et al., 1994) to calculate the friction force and losses in this study.

2.4.1. Thrust bearing

As shown inFig. 2(a), the thrust bearing is used to support against the resultant axial force F_a and turning moment M. Several models have been investigated in literatures (Kulkarni, 1990; Sato et al., 2004; Akei et al., 2006; Oku et al., 2008). A rigid-body wobbling model (Kulkarni, 1990; Akei et al., 2006) with hydrodynamic lubrication theory is adopted in this developed STC model. The definitions of relevant parameters are showed in Fig. 2(b). By assuming sufficient circulation of lubricant through the thrust bearing and the steady temperature, the Reynolds equation, including the wedge and squeeze terms for generating the pressures on the circular thrust surface, can be expressed in cylindrical coordinates as:

$$\frac{1}{R}\frac{\partial}{\partial R}\left(RH^3\frac{\partial p}{\partial R}\right)+\frac{1}{R^2}\frac{\partial}{\partial \Theta}\left(H^3\frac{\partial p}{\partial \Theta}\right)=6\mu\left(\frac{1}{R}\frac{\partial}{\partial R}(RHU_R)+\frac{1}{R}\frac{\partial}{\partial \Theta}(HU_\Theta)+2\frac{\partial H}{\partial t}\right) \quad (11)$$

The oil-film clearance H between the tilting orbiting scroll and thrust surface is

$$H = H_0 - \tan\alpha(R\sin(\Theta+\beta) - r_{ob}\cos(\theta-\beta)) \quad (12)$$

where H_0 is the nominal oil-film clearance (shown in Fig. 2(c)), α is the tilting angle and β is the directional tilting angle. The surface velocities and velocity derivatives of the orbiting scroll can be simplified as:

$$U = r_{ob}\cdot\omega; \quad \begin{cases} U_R = U\cos(\Theta+\theta); & \dfrac{\partial U_R}{\partial R} = 0 \\ U_\Theta = -U\sin(\Theta+\theta); & \dfrac{\partial U_\Theta}{\partial \Theta} = -U\cos(\Theta+\theta) \end{cases} \quad (13)$$

The following assumptions simplify the squeezing effect:

$$\dot{H}_0 = 0; \quad \dot{\alpha} = 0; \quad \dot{\beta} = \dot{\theta} = \omega$$
$$\frac{\partial H}{\partial t} = \frac{\partial H}{\partial \Theta}\omega \quad (14)$$

The Reynolds equation (11) is approximated by the finite difference operators and the successive over-relaxation (SOR) method is used as solution approach and the suction pressure is set as the boundary condition of the thrust surface. Once the pressure distribution is known, the force and moment from the lubrication oil can be integrated as

$$F_a' = \int_0^{2\pi}\int_{R_i}^{R_o} p\cdot R dR d\Theta \quad (15)$$

$$M_x' = \int_0^{2\pi}\int_{R_i}^{R_o} p\cdot R\sin\Theta\cdot R dR d\Theta; \quad M_y' = \int_0^{2\pi}\int_{R_i}^{R_o} p\cdot R\cos\Theta\cdot R dR d\Theta$$
$$M' = \sqrt{M_x'2 + M_y'2}; \quad \beta' = \tan^{-1}\left(\frac{M_y'}{M_x'}\right) \quad (16)$$

By equating the force and moment in equations (7), (15) and (9), (16), there are two simultaneous equations with two unknowns H_0 and α, and the Newton–Raphson method is used to solve the equations. Then the friction force $F_{f,th}$ and the frictional losses P_{th} are derived as below:

$$F_{f,th} = \int_0^{2\pi}\int_{R_i}^{R_o} \mu\frac{R^2\omega}{H} dR d\Theta$$
$$P_{th} = F_{f,th}\cdot U \quad (17)$$

Finally the average frictional losses of thrust bearing can be calculated.

2.4.2. Journal bearings

For journal bearing, selection of the inside diameter D_b, the clearance C_b and the length L_b can decide its frictional characteristics. In order to estimate the frictional losses, the numerical model utilizing mobility method for journal bearings (Booker, 1971; Geonka, 1984) is used and the frictional force becomes

$$F_{f,b} = \frac{F_b C_b \varepsilon}{D_b}\sin\Phi + \frac{2\pi\mu\omega L_b}{C_b(1-\varepsilon^2)^{0.5}}\left(\frac{D_b}{2}\right)^2 \quad (18)$$

where ε is the eccentricity ratio and Φ is the phase difference from eccentric and load direction. The frictional losses P_b are

$$P_b = F_{f,b}\cdot\frac{D_b}{2}\cdot\omega \quad (19)$$

Then the average frictional losses of the journal bearings can be calculated.

2.5. Simulation and experiments

The STC simulation model is programmed by using C++ combined with "*REFPROP 7*". The inputs include scroll geometry, related mechanisms, operating conditions and motor Torque-Efficiency-Power curves (as shown in Fig. 2(d)) from dynamometer test for specified speed used in this paper. The leakage model is included in the polytropic compression and discharge process and then is solved with the 4th Runge–Kutta

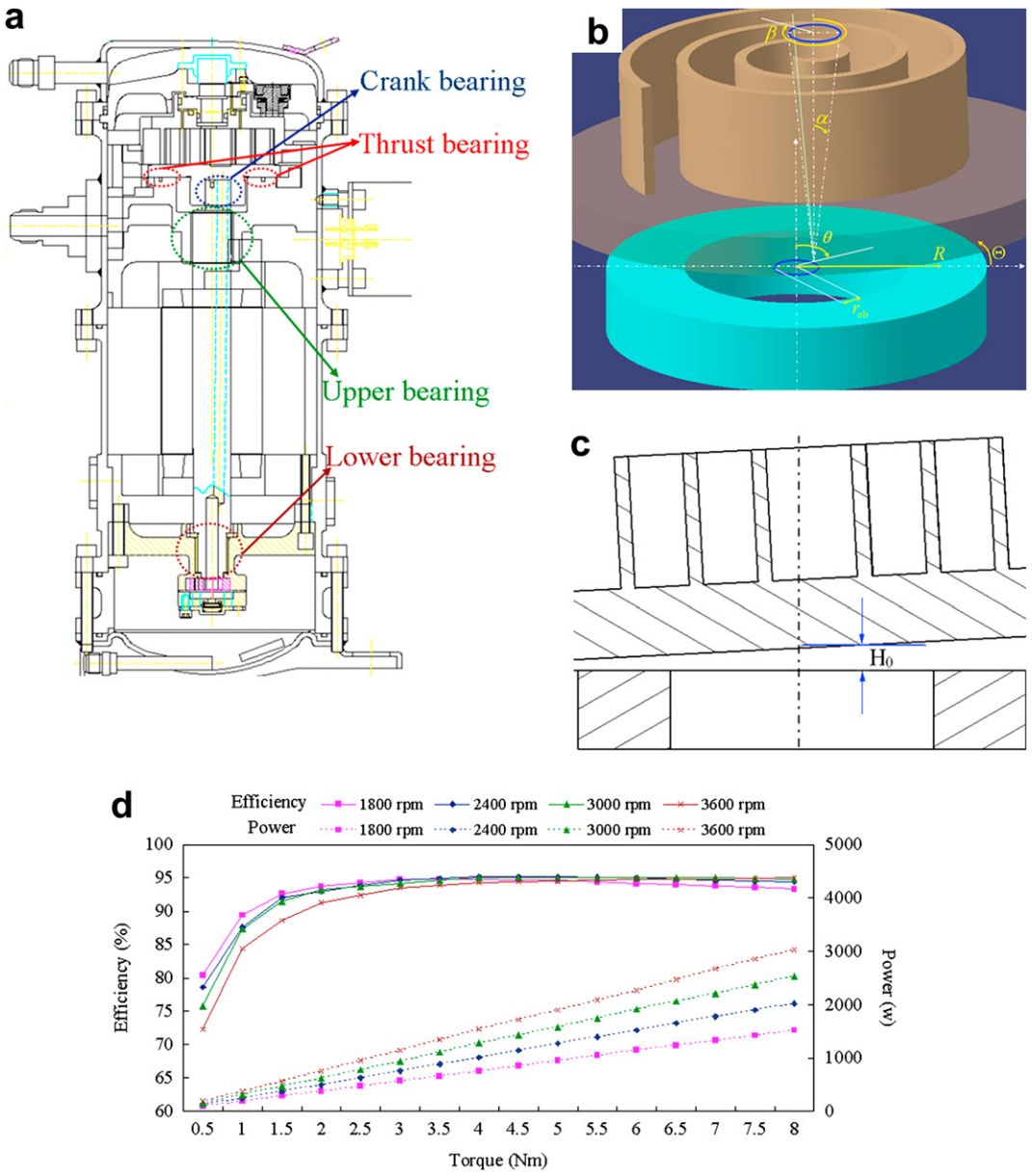

Fig. 2 – Bearing components (a) schematic of the three journal bearings and the thrust bearing (b) parameters of the thrust bearing (c) nominal height of oil-film (d) motor torque-efficiency-power for specified speed.

method. The dynamics and frictional losses of bearings are also calculated and finally the output results can be obtained.

One STC model with R_{22} refrigerant is used for comparisons between the simulation and experiment results. The characteristic parameters of the scroll pairs, and the two testing groups, different operating temperatures with constant speed (condition A) and same operating temperature with varying speed (condition B) are showed in Table 1. The STC model has been tested on a R_{22} calorimeter (specifications shown in Table 2) and the simulation and experiment results (0.35% expanded uncertainty in measured power and 0.12% expanded uncertainty in measured mass flow rate) are shown in Table 3.

For condition A, Table 3 shows the refrigerant mass flow rate, motor input power, volumetric efficiency (η_V) and compressor efficiency (η_C) which expressed as follows

$$\eta_V = \frac{\text{suction mass flow rate} - \text{leakage mass flow rate}}{\text{suction mass flow rate}}$$
$$\eta_C = \frac{P_{adiabatic}}{P_{electric}} = \frac{P_{adiabatic}}{P_{compression} + P_{frictional\ loss} + P_{motor\ loss}} \quad (20)$$

The relative errors to those values are all in the range of −3.3–3.5%. It is found that the lower temperature in operating conditions, the larger errors produced. Those errors may result from the deviation of the superheat in suction pipe and the evaluation of leakage gaps with linearity simplifications. Fig. 3(a) shows the various contributions to frictional losses from simulation at condition A and it is found that the greatest one is the frictional loss in thrust bearing (42–48%), followed by the upper bearing (22–25%), the crank bearing (18–21%), the lower bearing (6–8%) and others (3–5%) in turn. The ratio in various frictional losses is similar at all cases of condition A.

Table 1 – Parameters and operating conditions of the STC.

Characteristic parameters					
Basic circle radius (r_b)	2.062 (mm)				
Thickness of the scroll (t_h)	2.65 (mm)				
Roll angle of the scroll	20.25 (rad)				
Height of the scroll (h)	22 (mm)				
Discharge angle	3.79 (rad)				
End-plate diameter of the orbiting scroll	92 (mm)				
End-plate height of the orbiting scroll	7 (mm)				
End-plate diameter of the fixed scroll	112 (mm)				
End-plate height of the fixed scroll	12 (mm)				
Suction volume	3.39×10^{-5} (m^3)				
Volume ratio	3.25				
Condition A					
Motor revolution	60 rps				
Operating conditions	T_{evap} (°C)	T_{cond} (°C)	T_{suc} (°C)	p_{suc} (MPa)	p_{dis} (MPa)
A1	7.2	54.4	35	0.625	2.146
A2	7.2	48.9	18.3	0.625	1.894
A3	4.4	48.9	15.5	0.573	1.894
A4	−1.1	48.9	10	0.480	1.894
A5	−6.7	48.9	4.4	0.398	1.894
Condition B					
B1	30 rps				
B2	40 rps				
B3	50 rps				
Operating conditions	T_{evap} (°C)	T_{cond} (°C)	T_{suc} (°C)	p_{suc} (MPa)	p_{dis} (MPa)
	7.2	54.4	35	0.625	2.146

For condition B, the relative error of each index is in the range of −5.6–5.1%. Fig. 3(b) shows the contributions of frictional losses, and it is found that the lower motor speed, the lower amount of frictional losses and the contributive percentages of frictional losses are similar to those in condition A.

Though the simulation results show a little discrepancy with the experiments, the developed STC program with acceptable accuracy can be regarded as the basis for developing optimum design procedure.

3. Optimization solver

With advance in computer technology, computerized optimum procedures integrating the simulation program with the optimization algorithm can help designer to determine the suitable design parameters and get the optimum results within the prescribed constraints. In this study, the solver "*MOST*" is integrated into the STC simulation program to deal with the optimization problem.

3.1. *Formulation of optimization problem*

The solver has been developed by using constrained and gradient methods. The Sequential Quadratic Programming (SQP) method (Arora, 2004) has been selected as the kernel for the single objective, minimum type and continuous variables problem in this study. The formulation has been defined as follows:

Table 2 – Specifications of calorimeter for measuring STC performance.

Specifications		
Refrigerant	R_{22}	
Capacity range (Watt)	1500–12,000	
Description of system	According ISO917, design for fully automatic measurements	
Measuring method	The secondary refrigerant and liquid flow meter system	
Accuracy		
Deviation between the secondary refrigerant and liquid flow system	≤±4%	
Refrigerant flow-measuring instruments	≤±1%	
Speed measuring instruments	≤±0.75%	
Repeatability	≤±1%	
Control items	Range	Stability
p_{dis} of Compressor (MPa)	0.98–2.94	±0.01
p_{suc} of Compressor (MPa)	0.15–0.91	±0.015
T_{suc} of Compressor (°C)	−25–50	±0.5

Find a q-vector $\vec{x} = [x_1, x_2, x_3, \ldots x_q]^T$ of design variables to minimize an objective function

$$F(\vec{x}) = F(x_1, x_2, \ldots, x_q) \tag{21}$$

which is subject to the constraints

$$h_j(\vec{x}) = 0; \quad j = 1, 2, \ldots, p \tag{22}$$

$$g_i(\vec{x}) \le 0; \quad i = 1, 2, \ldots, m \tag{23}$$

the explicit bounds on design variables

$$x_{low}(k) \le x(k) \le x_{upp}(k); \quad k = 1, 2, \ldots, q \tag{24}$$

The $F(\vec{x})$ is the objective function and the design variables vector $\vec{x}$ represents the arguments varied in order to generate a better design. The constraints expressed by equations (22) and (23) define the feasible design space in conjunction with the design variable bounds specified by equation (24).

3.2. *Optimization procedure*

The optimization procedure is shown in Fig. 4. At the beginning stage, the design variables, objective function and constraint conditions, formulated and set as input data, are passed to the STC simulation program. Secondly, the program is executed and the output data can be obtained. The output data are then analyzed by the optimization solver. If the results do not satisfy the convergent criteria, a new group of design variables is derived by SQP method. This group will be returned to the simulation program as new input data to progress the procedure iteratively, until the convergent conditions are satisfied and finally the optimum result is found.

4. Optimization in reducing frictional losses

Owing to the frictional losses are mainly caused from the four bearing components, an optimization case to search the

Table 3 – Comparison between simulation and experimental results in different conditions.

	G (kg s^{-1})			Motor input (watt)			η_V (–)			η_C (–)		
	Sim.	Exp.	Err. (%)	Sim.	Exp.	Err. (%)	Sim.	Exp.	Err. (%)	Sim.	Exp.	Err. (%)
A1	2.532	2.528	0.1	2007	2014	−0.3	0.943	0.946	−0.3	0.749	0.754	−0.7
A2	2.715	2.707	0.3	1876	1866	0.5	0.923	0.931	−0.9	0.701	0.717	−2.2
A3	2.455	2.460	−0.2	1852	1812	2.2	0.908	0.915	−0.8	0.702	0.725	−3.3
A4	2.013	2.045	−1.5	1795	1737	3.3	0.882	0.877	0.6	0.683	0.706	−3.2
A5	1.643	1.665	−1.3	1731	1672	3.5	0.861	0.840	2.5	0.659	0.672	−1.9
B1	1.158	1.157	0.1	1034	1095	−5.6	0.878	0.907	−3.2	0.665	0.649	2.5
B2	1.601	1.595	0.4	1344	1374	−2.2	0.908	0.883	2.9	0.706	0.672	5.1
B3	2.075	2.083	−0.4	1681	1621	3.7	0.927	0.927	0.0	0.732	0.761	−3.8

optimum geometrical dimensions of the bearings for minimum frictional losses in STC is investigated.

4.1. *Selection of objective function and design variables*

The mechanical loss P_{mech} is selected as the objective function to be minimized. For the three journal bearings, two parameters, inner diameter (D) and length (L) are specified by design decisions. Hence, there are six design parameters selected for the three journal bearings. For the thrust bearing, the inner and outer diameters ($D_{i,th}$ and $D_{o,th}$) are considered as design variables. There are totally eight design variables of the problem and the objective function is mathematically defined as

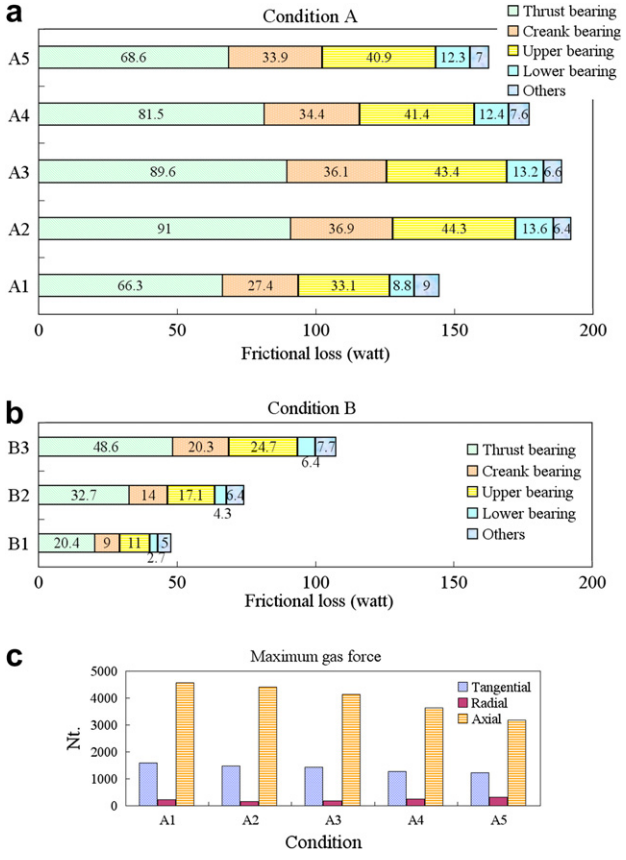

Fig. 3 – Frictional losses in (a) Condition A (b) Condition B (c) maximum loading in Condition A.

$$\text{Minimize } P_{mech}$$
$$\text{where } P_{mech} = F(\vec{x}) = F\left(L_{b,cr}, D_{b,cr}, L_{b,upp}, D_{b,upp}, L_{b,low}, D_{b,low}, D_{i,th}, D_{o,th}\right) \quad (25)$$

The lower and upper bounds of the design variables are expressed as

$$x_{low}(i) \le x(i) \le x_{upp}(i); \quad i = 1, 2, \ldots, 8 \quad (26)$$

Those bounds depend on the actual design considerations and space constraints for the developed STC model and values shown in Table 4 are specified to guarantee that the final design is feasible.

4.2. *Selection of constraint conditions*

When considering the behavior of hydrodynamic lubrication, the most important factor is that the full separating oil-film must be retained at running to ensure the mating surfaces are in the ideal operation with minimum wear and friction. So the minimum oil-film thickness should be greater than the roughness of the mating surfaces. The dimensionless film thickness commonly is defined as

$$\Lambda = \frac{h_{min}}{\overline{R}} = \frac{h_{min}}{\left(\overline{R}_a^2 + \overline{R}_b^2\right)^{0.5}} \quad (27)$$

where $\overline{R}_a$ and $\overline{R}_b$ represented the root-mean-square roughness of mating surfaces. With full-filling hydrodynamic lubrication, $\Lambda \ge 10$ must be satisfied(Khonsari and Booser, 2001), so the minimum thickness can be derived once the $\overline{R}_a$ and $\overline{R}_b$ are decided. In this study, both $\overline{R}_a$ and $\overline{R}_b$ are set to 0.4 μm, then the constraint h_{min} can be obtained as

$$h_{min} = \Lambda\left(\overline{R}_a^2 + \overline{R}_b^2\right)^{0.5} = 5.66\ \mu m \quad (28)$$

Therefore $h_{min} \ge 6$ μm was set as the first constraint for the four bearings.

Another consideration is the maximum oil-film pressure on contacted surfaces. For the four bearings, 10 MPa for allowable strength is set as upper limit of the constraint, i.e.

$$P_{max} \le 10\ \text{MPa} \quad (29)$$

The detailed constraint conditions are summarized in Table 4.

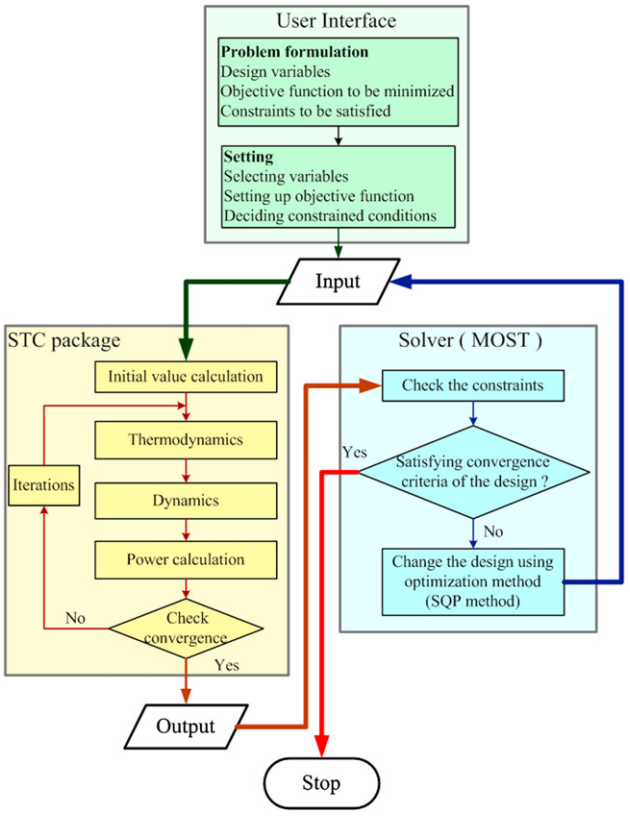

Fig. 4 – Flow chart of the optimization procedure.

5. Optimum results and discussions

5.1. *Selection of testing conditions*

Several testing conditions can be simulated in the optimization procedure. However, the severest condition should be adopted in order to promise that the final design of the STC can sustain well at all conditions. Fig. 3(c) shows several maximum gas forces act on the orbiting scroll during the orbiting cycle and it is found that the condition A1 has the greatest loading and is also the most frequent running condition. Hence condition A1 is selected as the testing condition in this optimization problem.

Table 4 – Bounds of design variables and constraints.

No.	Design variables	Lower bound (mm)	Upper bound (mm)	Constraint conditions No.	Constraints	Descriptions
1	$L_{b,cr}$	19.0	27.0	1	$p_{b,cr}$	≤10 Mpa
2	$D_{b,cr}$	21.5	29.5	2	$p_{b,upp}$	≤10 Mpa
3	$L_{b,upp}$	26.5	34.5	3	$p_{b,low}$	≤10 Mpa
4	$D_{b,upp}$	21.5	29.5	4	p_{th}	≤10 Mpa
5	$L_{b,low}$	19.0	27.5	5	$h_{b,cr}$	≥6 μm
6	$D_{b,low}$	16.0	22.0	6	$h_{b,upp}$	≥6 μm
7	$D_{o,th}$	75.0	90.0	7	$h_{b,low}$	≥6 μm
8	$D_{i,th}$	45.0	60.0	8	h_{th}	≥6 μm

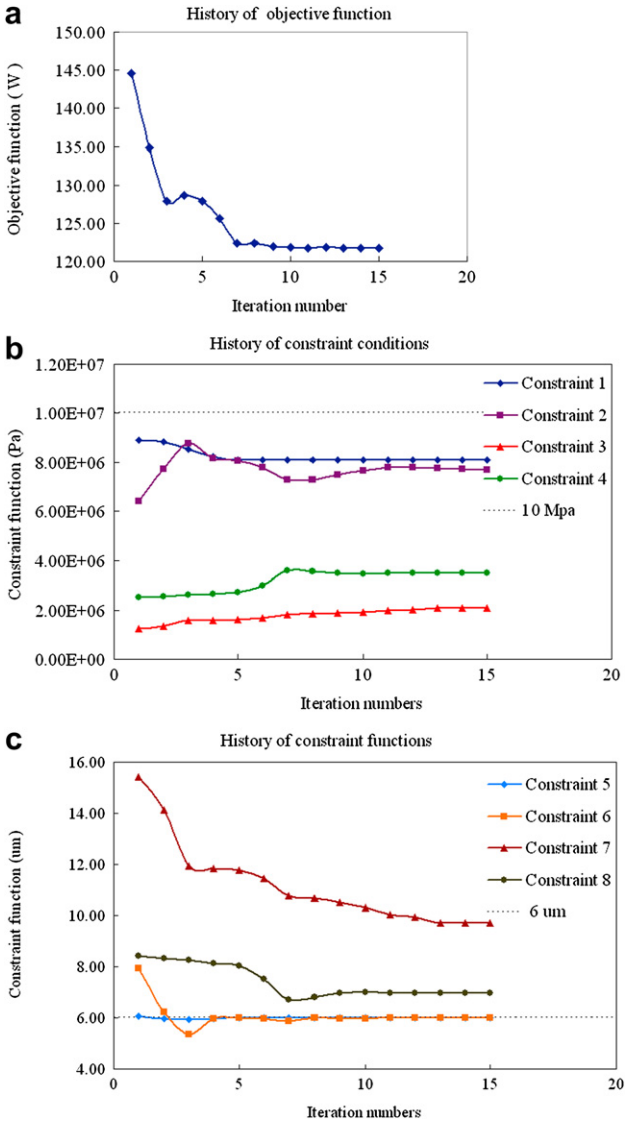

Fig. 5 – Iteration history (a) Objective function (b) Constraints 1–4 (c) Constraints 5–8.

5.2. *Optimum results*

The optimization search has been executed on a PC with 2.6 GHz Pentium C2D processor with 2 GB memory and it takes 2 h to finish. Fig. 5(a) shows that the objective function decreases during the iterations, and the mechanical loss reduces 16% (from 144.6 W to 121.7 W). The history of constrained conditions is shown in Fig. 5(b) and (c), it is found that all the constraints are satisfied. Moreover, two constraints, 5 and 6, are active. It reveals that the minimum film thickness of the crank and upper bearing ($h_{b,cr}$ and $h_{b,upp}$) have approached the limitation (6 μm). Table 5 shows the variation of design variables and respective power consumptions before and after the optimization. It is found that the frictional losses of each bearing are reduced in range of 11.4–38.1%.

Table 5 – Optimized results with design variables.

No.	Design variables	Initial (mm)	Optimized (mm)	Variation (%)
1	$L_{b,cr}$	23.00	27.00	17.4
2	$D_{b,cr}$	25.40	22.45	−11.6
3	$L_{b,upp}$	31.00	31.47	1.5
4	$D_{b,upp}$	25.40	22.05	−13.2
5	$L_{b,low}$	23.00	19.00	−17.4
6	$D_{b,low}$	18.95	16.00	−15.6
7	$D_{o,th}$	85.00	75.00	−11.8
8	$D_{i,th}$	55.00	45.00	−18.2

Results	Initial (watt)	Optimized (watt)	Variation (%)
Loss of thrust bearing	66.54	58.95	11.4
Loss of crank journal bearing	27.48	23.28	15.3
Loss of upper journal bearing	33.21	26.23	21.0
Loss of lower journal bearing	8.82	5.46	38.1
Others	8.55	7.78	9.0
Summation	144.6	121.7	15.8

5.3. *Discussions*

The results shows in Fig. 5(a), (c) and Table 5 imply that the design modification of crank and upper journal bearings reduce the frictional losses while the constraints of minimum oil-film thickness are met, so the decrease level of the losses is confined. Furthermore, the trend of smaller diameter of the crank and upper bearings can reduce the frictional losses. The design variables related to lower journal bearing ($L_{b,low}$ and $D_{b,low}$) finally locate at the lower bounds, it means that the shorter and narrower one can reduce the frictional losses without violating the specified constraints.

For the thrust bearing that contributed to the maximum power consumption in frictional losses, it is found that the related design variables ($D_{i,th}$ and $D_{o,th}$) are located at the lower bound of the design limitations. It is said that for the specified design bounds and constraint conditions, the smaller inner and outer diameter of the thrust bearing, the larger amount of frictional losses can be reduced. However, Table 5 shows that the variation ratio between initial and optimized reductive frictional losses of the thrust bearing (11.4%) is smaller than that of the three journal bearings (15.3–38.1%).

In addition, the maximum pressure constraints (constraint 1–4, shown in Fig. 5(b)) are not infringed by the design parameters of the three journal bearings and the thrust bearing during the optimization search. The constraints for the strength consideration do not affect the optimum search in this study, which indicated that the bearing materials may have broader selectivity.

After the optimum search of the STC, the simulated results of the new design in all testing conditions are shown in Fig. 6, and it is found that the frictional losses can be reduced in range of 14.1%–18.1%. It demonstrates that this design optimization procedure can help improve STC efficiency effectively.

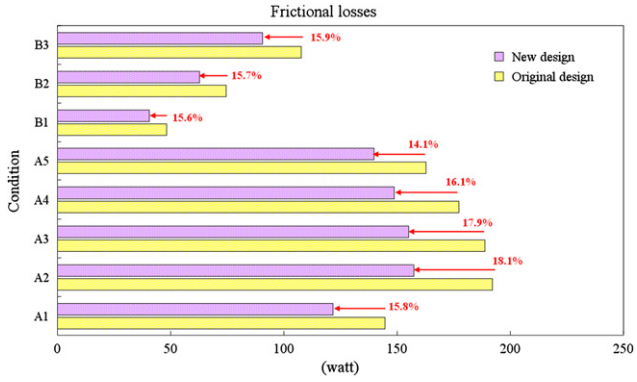

Fig. 6 – Frictional losses in all testing conditions.

6. Conclusions

This study has developed a computer procedure that integrated a general mathematical model of STC and the optimization solver "*MOST*" to progress the optimization research. An optimum problem in reducing frictional losses of bearing components, and fitting in with specified constraint conditions has been explored. Several aspects are summarized as below:

1. A mathematical model of STC has been developed and verified by the experiments with different testing conditions. An optimum solver has been combined with the model to progress design decision of constrained optimization problem.
2. The optimization results for a selected STC design problem shows that the frictional losses can be reduced in range of 14.1–18.1% at all testing conditions by new design group which is satisfied at the specified constraint conditions for one thrust and three journal bearings.
3. For the crank and upper journal bearings, the design modifications can reduce the frictional losses, but the constraints of minimum oil-film thickness for holding hydrodynamic lubrication can block the further decrease of the frictional losses. For the lower journal bearing, the shorter and narrower dimensions can reduce the frictional losses without violating the oil-film constraint. For the thrust bearing, the smaller inner and outer diameter of the thrust surface, the larger reduction in frictional losses with specified design constraints. Furthermore, the constraints of the maximum pressure that related to the strength consideration of all the bearings are satisfied in all iterations during optimization and these results signify wider space for material selection.
4. The integration between the parametric simulation model of STC and optimum solver in this study can be a useful procedure and as the basis to progress various STC design optimization problems.

Acknowledgments

The authors would like to express gratitude for financial support from the Energy & Environment Research

Laboratories, Industrial Technology Research Institute in Taiwan. The authors would also like to thank the National Center for High–Performance Computing in Taiwan for its facility support.

REFERENCES

Akei, M., Teng, H., Ignative, K.M., 2006. Analysis of scroll thrust bearing. In: Proceedings of International Compressor Engineering Conference at Purdue, C136.

Arora, J.S., 2004. Introduction to Optimum Design. McGraw-Hill.

Booker, J.F., 1971. Dynamically-loaded journal bearings: numerical application of the mobility method. Journal of Lubrication Technology, Transaction of the ASME, 168–176.

Chang, Y.C., Tsai, C.E., Tseng, C.H., Tarng, G.D., Chang, L.T., 2004. Computer simulation and experimental validation of scroll compressor. In: Proceedings of International Compressor Engineering Conference at Purdue, C016.

Chen, Y., Halm, N.P., Groll, E.A., Braun, J.E., 2002. Mathematical modeling of scroll compressors—part I: compression process modeling. Int. J. of Refrigeration 25, 731–750.

Etemad, S., Nieter, J.J., 1989. Design optimization of the scroll compressor. International Journal of Refrigeration 12, 146–150.

Geonka, P.K., 1984. Analytical curve fits for solution parameters of dynamically loaded journal bearings. Journal of Tribology 106, 421–428.

Ishii, N., Yamamoto, S., Muramatsu, S., Yamamura, M., Takahashi, M., 1992. Optimum combination of parameters for high mechanical efficiency of a scroll compressor. In: Proceedings of International Compressor Engineering Conference at Purdue, pp. 118a1–118a8.

Ishii, N., Yamamura, M., Muramatsu, S., Yamada, S., Takahashi, M., 1994. A study on high mechanical efficiency of a scroll compressor with fixed cylinder diameter. In: Proceedings of International Compressor Engineering Conference at Purdue, pp. 677–682.

Ishii, N., Sakai, M., Sano, K., Yamamoto, S., Otokura, T., 1996. A fundamental optimum design for high mechanical and volumetric efficiency of compact scroll compressor. In: Proceedings of International Compressor Engineering Conference at Purdue, pp. 639–644.

Khonsari, M.M., Booser, E.R., 2001. Applied Tribology—Bearing Design and Lubrication. John-Wiley.

Kulkarni, S.S., 1990. Thrust bearing design under laminar conditions. In: Proceedings of International Compressor Engineering Conference at Purdue, pp. 327–332.

Lemmon, E.W., McLinden, M.O., Huber, M.L., 2002. REFPROP 7.0. NIST, MD, USA.

Morishita, E., Sugihara, M., Inaba, T., Nakamura, T., 1984. Scroll compressor analytical model. In: Proceedings of International Compressor Engineering Conference at Purdue, pp. 487–495.

Morishita, E., Sugihara, M., Nakamura, T., 1986. Scroll compressor dynamics (1st report, the model for the fixed radius crank). Bulletin of JSME 29 (248), 476–482.

Nieter, J.J., Gagne, D.P., 1992. Analytical modeling of discharge flow dynamics in scroll compressors. In: Proceedings of International Compressor Engineering Conference at Purdue, pp. 85–94.

Ooi, K.T., 2005. Design optimization of a rolling piston compressor for refrigerators. Applied Thermal Engineering 25, 813–829.

Oku, T., Ishii N., Anami K., Knisely C. W., Sawai K., Morimoto T., Hiwata A., 2008. Theoretical Model of Lubrication Mechanism in the Thrust Slide-Bearing of Scroll Compressors. HVAC & R Research 14 (2), 239–258.

Park, Y.C., Kim, Y., Cho, H., 2002. Thermodynamic analysis on the performance of a variable speed scroll compressor with refrigerant injection. Int. J. of Refrigeration 25, 1072–1082.

Sato, H., Itoh, T., Kobayashi, H., 2004. Frictional characteristics of thrust bearing in scroll compressor. In: Proceedings of International Compressor Engineering Conference at Purdue, C027.

Schein, C., Radermacher, R., 2001. Scroll compressor simulation model. Journal of Engineering for Gas Turbines and Power, Transactions of the ASME 123, 217–225.

Tseng, C.H., 1996. MOST 1.1. Department of Mechanical Engineering of National Chiao Tung University, Taiwan.

Tseng, C.H., Chang, Y.C., 2006. Family design of scroll compressors with optimization. Applied Thermal Engineering 26, 1074–1086.